

Geophysical Research Letters[®]

RESEARCH LETTER

10.1029/2023GL107703

Key Points:

- Diurnal changes in carbonate chemistry occur, but cannot fully explain the unexpectedly high $\delta^{13}\text{C}_{\text{carb}}$ values of ooid sand on Caicos Platform
- The ^{13}C Suess effect is primarily responsible for the offset between predicted and expected $\delta^{13}\text{C}_{\text{carb}}$ values on Caicos Platform
- Consideration of the ^{13}C Suess effect is critical for interpretations of modern carbonate sediments as analogs for the rock record

Supporting Information:

Supporting Information may be found in the online version of this article.

Correspondence to:

E. J. Trower,
lizzy.trower@colorado.edu

Citation:

Trower, E. J., Hibner, B. M., Lincoln, T. A., Dodd, J. E., Hagen, C. J., Cantine, M. D., & Gomes, M. L. (2024). Revisiting elevated $\delta^{13}\text{C}$ values of sediment on modern carbonate platforms. *Geophysical Research Letters*, 51, e2023GL107703. <https://doi.org/10.1029/2023GL107703>

Received 8 DEC 2023

Accepted 22 JUL 2024

Author Contributions:

Conceptualization: Elizabeth J. Trower, Cedric J. Hagen, Marjorie D. Cantine, Maya L. Gomes

Funding acquisition: Elizabeth J. Trower, Marjorie D. Cantine, Maya L. Gomes

Investigation: Elizabeth J. Trower, Brianna M. Hibner, Tyler A. Lincoln, Jacqueline E. Dodd, Cedric J. Hagen, Marjorie D. Cantine, Maya L. Gomes

Methodology: Elizabeth J. Trower, Brianna M. Hibner, Tyler A. Lincoln, Jacqueline E. Dodd

Project administration: Elizabeth J. Trower

© 2024. The Author(s).

This is an open access article under the terms of the [Creative Commons Attribution-NonCommercial-NoDerivs License](#), which permits use and distribution in any medium, provided the original work is properly cited, the use is non-commercial and no modifications or adaptations are made.

Revisiting Elevated $\delta^{13}\text{C}$ Values of Sediment on Modern Carbonate Platforms



Elizabeth J. Trower¹ , Brianna M. Hibner¹, Tyler A. Lincoln¹ , Jacqueline E. Dodd², Cedric J. Hagen¹ , Marjorie D. Cantine³, and Maya L. Gomes² 

¹Department of Geological Sciences, University of Colorado Boulder, Boulder, CO, USA, ²Department of Earth and Planetary Sciences, Johns Hopkins University, Baltimore, MD, USA, ³Department of Earth and Space Sciences, University of Washington, Seattle, WA, USA

Abstract The measured carbon isotopic compositions of carbonate sediments ($\delta^{13}\text{C}_{\text{carb}}$) on modern platforms are commonly ^{13}C -enriched compared to predicted values for minerals forming in isotopic equilibrium with the dissolved inorganic carbon (DIC) of modern seawater. This offset undermines the assumption that $\delta^{13}\text{C}_{\text{carb}}$ values of analogous facies in the rock record are an accurate archive of information about Earth's global carbon cycle. We present a new data set of the diurnal variation in carbonate chemistry and seawater $\delta^{13}\text{C}_{\text{DIC}}$ values on a modern carbonate platform. These data demonstrate that $\delta^{13}\text{C}_{\text{carb}}$ values on modern platforms are broadly representative of seawater, but only after accounting for the recent decrease in the ^{13}C value of atmospheric CO_2 and shallow seawater DIC due to anthropogenic carbon release, a phenomenon commonly referred to as the ^{13}C Suess effect. These findings highlight an important, yet overlooked, aspect of some modern carbonate systems, which must inform their use as ancient analogs.

Plain Language Summary Carbon isotope values of carbonate minerals ($\delta^{13}\text{C}_{\text{carb}}$) are an important archive of information about Earth's carbon cycle in the geological past. To interpret this archive, we must understand how to identify carbonate rocks in which preserved $\delta^{13}\text{C}_{\text{carb}}$ values are representative of global trends. This effort has long been challenged by a puzzling observation in modern shallow water carbonate-producing environments like the Bahamas: $\delta^{13}\text{C}_{\text{carb}}$ values of some sediments in these settings are higher than we predict they should be relative to $\delta^{13}\text{C}$ values of seawater. These unexpectedly high $\delta^{13}\text{C}_{\text{carb}}$ values potentially suggest that $\delta^{13}\text{C}_{\text{carb}}$ values in carbonate rocks deposited in similar environments reflect local, rather than global processes, questioning the application of this important and long-used tool. We measured hourly changes in seawater chemistry on a shallow marine carbonate platform and observed evidence of two key effects: (a) daily variation in $\delta^{13}\text{C}$ values driven by photosynthesis, and (b) the recent change in the ^{13}C value of atmospheric CO_2 and shallow seawater due to anthropogenic carbon release (the ^{13}C Suess effect). Our data show that $\delta^{13}\text{C}_{\text{carb}}$ values of shallow marine carbonates are broadly representative of seawater, but only if we account for the ^{13}C Suess effect.

1. Introduction

Carbon isotopic compositions of carbonate rocks ($\delta^{13}\text{C}_{\text{carb}}$) are a primary tool used to reconstruct global carbon cycle changes and establish temporal relationships between spatially distant sedimentary records in the geological past (Knoll et al., 1986; Kump & Arthur, 1999; Zachos et al., 2001). Modern carbonate platform sediments—and their carbon isotopes—are commonly used as analogs for interpreting the carbonate rock record and the Earth's carbon cycle in deep time (Oehlert & Swart, 2014; Purkis et al., 2012, 2015; Swart & Eberli, 2005; Swart et al., 2009). The assumption that the $\delta^{13}\text{C}_{\text{carb}}$ values of ancient sediments faithfully record the carbon isotope compositions of dissolved inorganic carbon (DIC) in ancient seawater ($\delta^{13}\text{C}_{\text{DIC}}$) is foundational to many studies of Earth's carbon cycle in deep time.

However, this premise is complicated by studies of modern carbonate platform sediments highlighting variability in the $\delta^{13}\text{C}_{\text{carb}}$ record of recent sediments unrelated to global carbon perturbations. These include previously unrecognized diagenetic effects (Ahm et al., 2018; Higgins et al., 2018; Smith & Swart, 2022; Swart, 2015; Swart & Oehlert, 2018) and facies-driven controls on $\delta^{13}\text{C}_{\text{carb}}$ values (Geyman & Maloof, 2021; Ingalls et al., 2020). Such observations challenge classic paradigms of interpreting the geological record, throwing into question the meaning of more than 3 billion years of $\delta^{13}\text{C}_{\text{carb}}$ records and the relevance of a tool extensively used for the better part of a century to track change in the geobiosphere. In particular, it may be difficult to reconcile this

Software: Elizabeth J. Trower, Marjorie D. Cantine

Visualization: Elizabeth J. Trower, Brianna M. Hibner, Marjorie D. Cantine

Writing – original draft: Elizabeth J. Trower

Writing – review & editing: Elizabeth J. Trower, Brianna M. Hibner, Tyler A. Lincoln, Jacqueline E. Dodd, Cedric J. Hagen, Marjorie D. Cantine, Maya L. Gomes

foundational assumption with the long-standing observation that, in modern shallow marine carbonate platform sediments across the Lucayan Archipelago, $\delta^{13}\text{C}_{\text{carb}}$ values are higher than predicted if their composition were determined by precipitation in isotopic equilibrium with modern seawater $\delta^{13}\text{C}_{\text{DIC}}$ values.

A recently proposed explanation is that this offset between observed and predicted $\delta^{13}\text{C}_{\text{carb}}$ values results from a phenomenon termed the “diurnal engine” (Geyman & Maloof, 2019). The diurnal engine model suggests that cumulative $\delta^{13}\text{C}_{\text{carb}}$ values for precipitated minerals that are higher than expected for minerals precipitated in equilibrium with mean DIC are caused by diurnal variations in water chemistry. During the daytime, photosynthesis-dominated carbon cycling drives increases in $\delta^{13}\text{C}_{\text{DIC}}$ values and the carbonate mineral saturation state (Ω), resulting in more rapid carbonate precipitation. At nighttime, heterotrophy-dominated carbon cycling dominates, driving decreases in $\delta^{13}\text{C}_{\text{DIC}}$ and Ω values. The magnitude of this predicted $\delta^{13}\text{C}_{\text{carb}}$ offset is 4–7‰ in highly productive settings like zooxanthellate coral reefs (Geyman & Maloof, 2019).

An alternative explanation for the observed, higher-than-predicted offset between the $\delta^{13}\text{C}_{\text{carb}}$ values of modern carbonate platform sediments and modern DIC is that modern DIC is not the proper reference frame for time-averaged carbonate sediments. Modern seawater DIC is affected by the input of isotopically light carbon to the atmosphere from anthropogenic fossil fuel emissions (Eide et al., 2017) and thus $\delta^{13}\text{C}_{\text{DIC}}$ values have been decreasing over the course of the industrial revolution, a process first recognized for ^{14}C (Suess, 1955) and later extended to also include a ^{13}C Suess effect, as defined by Keeling (1979). “Modern” platform-top sediments are typically defined as the material at the modern sediment-water interface, even though this material can commonly include carbonate precipitated over hundreds to a few thousands of years (Beaupré et al., 2015; Duguid et al., 2010). This mismatch in timescales means that $\delta^{13}\text{C}_{\text{carb}}$ values might partially or entirely reflect pre-industrial DIC with a higher pre-industrial $\delta^{13}\text{C}_{\text{DIC}}$ value. For example, radiocarbon data from ooids representing locations across the Lucayan Archipelago demonstrate that the majority of the carbonate in these ooids is pre-industrial in age and therefore should not be compared with $\delta^{13}\text{C}_{\text{DIC}}$ values of modern seawater. Thus, the observed, higher-than-predicted offset could be, in whole or in part, the results of a previously overlooked phenomenon.

The ^{13}C Suess effect could also provide a new explanation for puzzling patterns in the $\delta^{13}\text{C}_{\text{carb}}$ values of ooid sediment across the Lucayan Archipelago: using sequential dissolution to compare $\delta^{13}\text{C}$ values in outer versus inner cortices in ooid sands, Duguid et al. (2010) observed that the outermost cortices (the youngest part of the ooid, represented by the first 10% of dissolution) had the lowest $\delta^{13}\text{C}_{\text{carb}}$ values, while the inner parts of the cortex (>10% of dissolution) had higher $\delta^{13}\text{C}_{\text{carb}}$ values than expected for aragonite precipitating in isotopic equilibrium with modern seawater. They hypothesized that cements filling endolithic microborings might have elevated $\delta^{13}\text{C}_{\text{carb}}$ values due to photosynthesis (i.e., the diurnal engine effect). However, their analyses did not directly show that cements filling microborings have distinct $\delta^{13}\text{C}_{\text{carb}}$ values relative to the adjacent cortex, nor did they demonstrate that such cements are volumetrically significant enough to have such a significant effect on bulk $\delta^{13}\text{C}_{\text{carb}}$ values. We hypothesize that the ^{13}C Suess effect could explain this pattern.

We designed a study to constrain the roles of diurnal carbon cycling and the ^{13}C Suess effect for the Caicos Platform, a grainy, wave-dominated carbonate platform in the Turks and Caicos Islands at the southeastern end of the Lucayan Archipelago (Figure 1). Reefs primarily occur along the margins of the Caicos Platform (Logan & Sealey, 2013). The wave-swept interior is dominated instead by aragonite sand with sparse green algae (primarily *Penicillus* and *Halimeda*) and isolated patch reefs (Dravis & Wanless, 2017). One might intuitively expect this environment to have a lower photosynthetic forcing (κ_p) than reef-dominated environments. Ooid sand from the active shoal on the Caicos Platform has bulk $\delta^{13}\text{C}_{\text{carb}}$ values of 4.69–4.78‰ (Trower et al., 2018). This $\delta^{13}\text{C}_{\text{carb}}$ value is ca. 1.5‰ heavier than predicted for aragonite precipitated in equilibrium with modern DIC on the platform. In contrast, the outermost cortices of Ambergris shoal ooids have $\delta^{13}\text{C}_{\text{carb}}$ values ranging from 3 to 4‰ (Duguid et al., 2010), which overlap with predicted $\delta^{13}\text{C}_{\text{carb}}$ values, but could still incorporate a modest diurnal engine effect. Modern Caicos Platform water has $\delta^{13}\text{C}_{\text{DIC}} = 0.8\text{\textperthousand}$ (Present et al., 2021; Trower et al., 2018), which falls within the range of modern ^{13}C -Suess-effect-impacted seawater $\delta^{13}\text{C}_{\text{DIC}}$ values (Eide et al., 2017); and the carbon isotope fractionation associated with aragonite precipitation at ca. 25°C is $2.7 \pm 0.6\text{\textperthousand}$ (Romanek et al., 1992). To quantify the effect of diurnal carbon cycling on the carbonate chemistry and $\delta^{13}\text{C}_{\text{DIC}}$ values of Caicos Platform seawater, we collected a time series of water samples a platform site adjacent to the shore of Little Ambergris Cay and consistent with the “algae-stabilized subtidal” environment described by Trower et al. (2018).

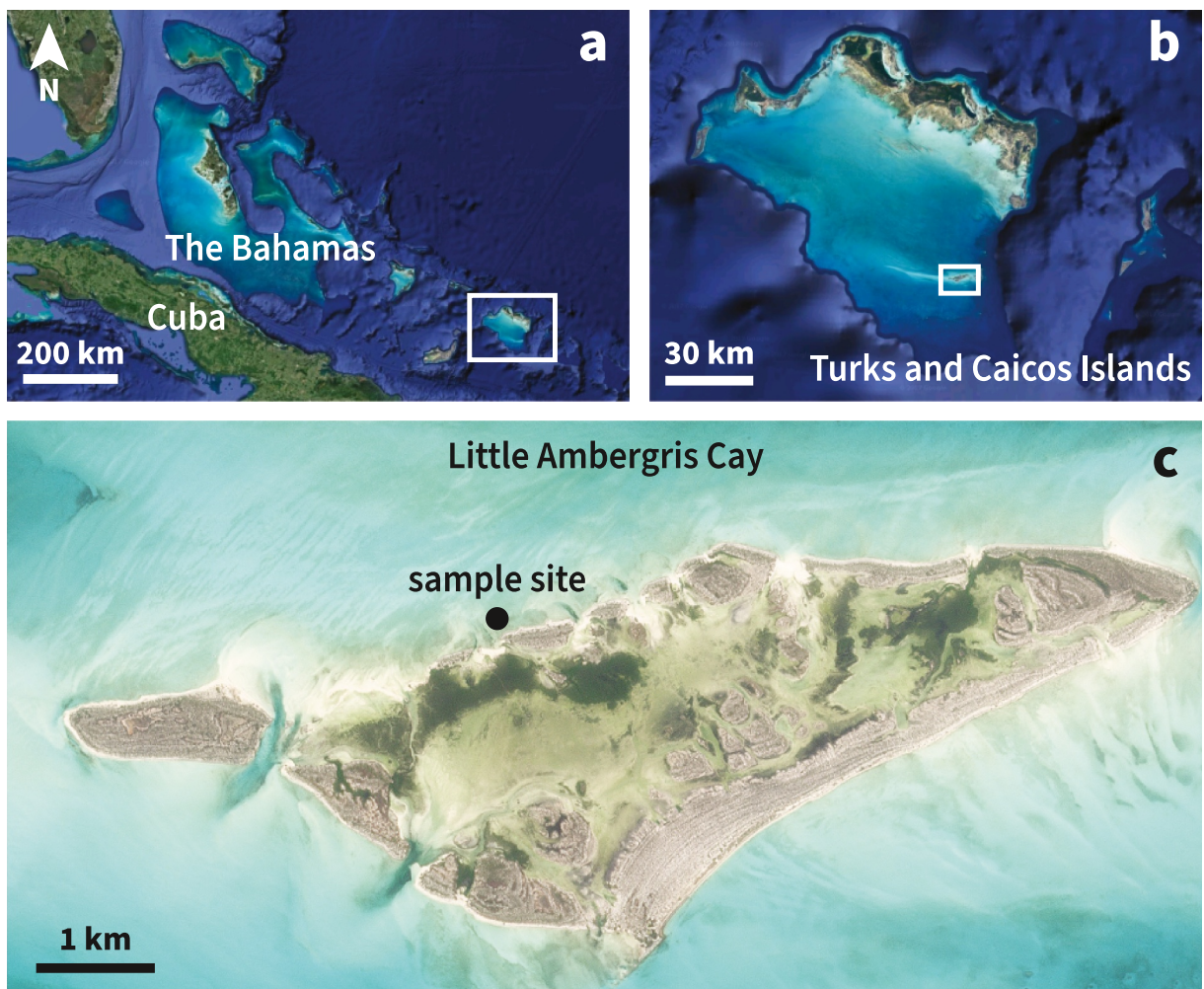


Figure 1. Location maps of sampling site. (a) Satellite image of the Lucayan Archipelago, with panel (b) inset shown in white box. (b) Satellite image of the Turks and Caicos Islands, with panel (c) inset shown in white box. (c) Satellite image of Little Ambergris Cay from 27 July 2023, with sample site shown with black circle. Satellite imagery from Google Earth (panels a and b) and Planet (panel c).

2. Materials and Methods

We collected platform water samples at 1-hr intervals over a duration of 24 hr. Although the platform water sampling site was located relatively close to Little Ambergris Cay for logistical reasons, the site location was chosen to minimize the influence from the adjacent tidal channel. It is also unlikely that this location is influenced by meteoric water because the range of mean precipitation-evaporation is 0 to -6 mm/day, with the majority of the <1 m/yr rainfall occurring during the peak of hurricane season (September–October) (Jury, 2013). We collected platform samples hourly from 09:21 on 28 July 2023 to 08:21 on 29 July 2023. Civil dusk (3.4 lux) occurred at 19:53 on 28 July 2023, and civil dawn (3.4 lux) occurred at 05:52 on 29 July 2023 (Figure S1 in Supporting Information S1). Fieldwork and sample collection was carried out under Scientific Research Permit 2023-05-23-25 from the Department of Environmental and Coastal Resources (DECR) of the Turks and Caicos Islands.

For each timepoint, we measured pH and temperature in situ, and collected three samples of water filtered with a $0.22\text{ }\mu\text{m}$ syringe filter: (a) 1.5 mL for characterization of major ion concentrations in a microcentrifuge tube; (b) 1 mL for characterization of $\delta^{13}\text{C}_{\text{DIC}}$ in an Exetainer that was evacuated, flushed with He, and acidified; and (c) 50 mL for alkalinity titration in a 50 mL centrifuge tube sealed immediately with Parafilm. To compare water chemistry data with light levels, we deployed a HOBO Pendant MX Temperature/Light Data Logger for the duration of the experiment (Figure S1 in Supporting Information S1). We placed the light meter in a separate but

nearby location so light data would not be contaminated by contributions from headlamp light during nighttime sampling points.

Major ion concentration samples were sent to the Laboratory for Isotopes and Metals in the Environment (LIME) facility at Pennsylvania State University for analysis. Concentrations of major cations (Ca, K, Mg, Na) were measured via a Thermo iCAP 7,400 Inductively Coupled Plasma Emission Mass Spectrometer (ICP-AES). Major anion (Cl, SO₄) concentrations were measured via a Dionex ICS 2,100 Ion Chromatography (IC) System. Synthetic standards from High Purity Standards were used to calibrate ICP-AES and IC results. DIC samples were analyzed via a Thermo Delta V continuous-flow stable isotope ratio mass spectrometer attached to a gas bench device in the University of Colorado (CU) Boulder Earth Systems Stable Isotope (CUBES-SIL) Core Facility. A suite of carbonate standards (IAEA-603, USGS-44, YULE, and NBS-18) in Extainer vials were flushed with helium for 10 min before adding 1 mL of boiled water and 0.2 mL of boiled 85% phosphoric acid. Sample δ¹³C values were corrected for a linearity then scaled using a four-point scale correction. Alkalinity was measured by titration with a ThermoFisher Orion Star T910 autotitrator using 0.1 M HCl. Samples from time-points at 21:17, 23:24, and 00:20 were excluded from our analysis because of anomalies with pH and/or alkalinity measurements.

We calculated Ω_{ar} values using both CO2SYS (Sharp et al., 2023) and PHREEQC (Parkhurst & Appelo, 2013). The absolute values of aragonite saturation state (Ω_{ar}) estimates varied somewhat between CO2SYS and PHREEQC, but the magnitudes of change and directions of change were the same (Data Set S1). CO2SYS values are shown in data figures so that they are directly comparable to diurnal engine model curves because the diurnal engine model uses CO2SYS to calculate carbonate speciation for each timestep. Calculated Ω_{ar} values were used to estimate cumulative δ¹³C_{carb} values. We compared results for the empirical rate constant based on field data (Geyman & Maloof, 2019) with an empirical rate constant based on experiments (Burton & Walter, 1987) (Figure S2 in Supporting Information S1).

3. Results

During our sampling interval, we observed the following ranges of carbonate chemistry parameters in Caicos Platform water: pH ranged from 7.97 to 8.18 (mean 8.09); alkalinity ranged from 2.36 to 2.41 mequiv/kg (mean 2.38 mequiv/kg) [DIC] ranged from 1.97 to 2.12 mmol/kg (mean 2.04 mmol/kg); pCO₂ ranged from 270 to 497 μatm (mean 360 μatm); and Ω_{ar} ranged from 3.4 to 4.9 (mean 4.2) (Figure 2, Figure S3 in Supporting Information S1, Data Set S1). The average platform water temperature (26.8°C, Data Set S1) is consistent with sea surface temperatures on Caicos Platform, which vary between 26 and 28°C (Jury, 2013). δ¹³C_{DIC} values ranged from 0.30 to 1.21‰ (mean 0.70‰) (Figure 2, Data Set S1). Ranges of pH, alkalinity [DIC], pCO₂, Ω_{ar}, and δ¹³C_{DIC} values were consistent with analogous observations of Caicos Platform water from sites adjacent to Little Ambergris Cay in 2017 during typical daytime fieldwork hours (ca. 10:00–16:00) (Trower et al., 2018) (Figure 2). Our observations show coherent shifts in terms of decreasing [DIC] and pCO₂, and increasing pH, Ω_{ar}, and δ¹³C_{DIC} values from 07:21–18:24 (light level ca. 20,000 lux) (Figure 2). In contrast, variations in alkalinity were small in magnitude and appeared more related to tides than changing light levels (Figure 2b). To assess whether our data could be described by the diurnal engine model, we estimated a κ_p value of 139 μmol/kg following the method described in Geyman and Maloof (2019) and applied this value to the diurnal engine model (Figure S4 in Supporting Information S1). We used a simple sinusoid curve to describe the shape of photosynthetic forcing because we considered this a better test than fitting the forcing curve to our data, which is influenced by both diurnal and tidal changes (Figure S4 in Supporting Information S1). Diurnal variations in our Caicos Platform seawater data are consistent with the premise that short-term variations in δ¹³C_{DIC} values are controlled by photosynthesis (Figure 2).

We used calculated platform Ω_{ar} values to estimate carbonate precipitation rates across the diurnal cycle, from which we calculated cumulative δ¹³C_{carb} values (weighted by the relative precipitation rate at each time point). This calculation suggested a cumulative δ¹³C_{carb} value (3.46‰) that is slightly higher, but within the range of typical uncertainty of δ¹³C_{carb} analyses (~0.1‰), relative to the δ¹³C_{carb} value that would be predicted from the mean δ¹³C_{DIC} value (3.40‰) (Figure S2 in Supporting Information S1). This predicted δ¹³C_{carb} value is significantly lower than bulk δ¹³C_{carb} values of modern ooid shoal sediment (Trower et al., 2018), but is similar to δ¹³C_{carb} values reported from the exterior cortices of Ambergris shoal ooids, which precipitated in the past 60 years (Duguid et al., 2010).

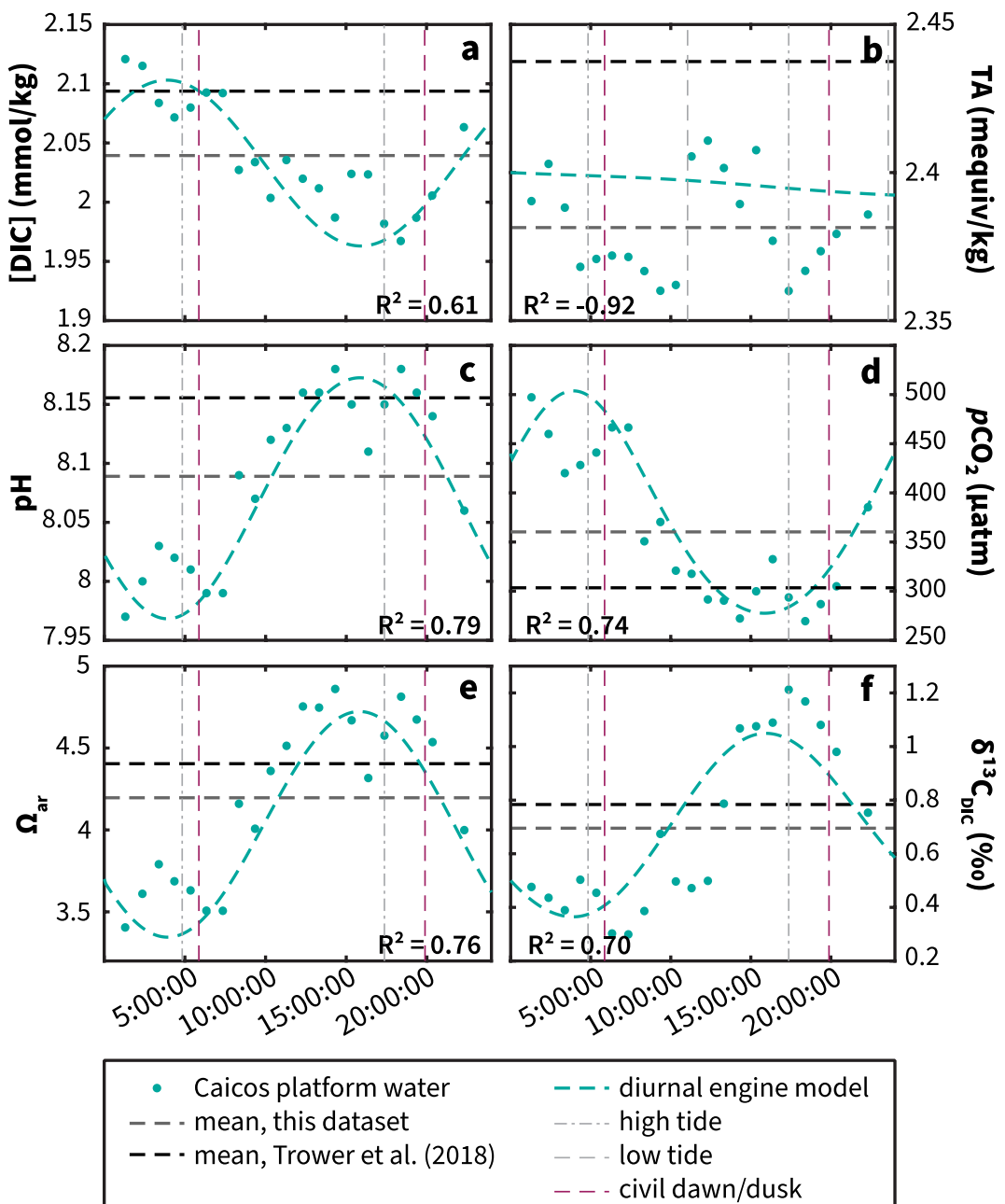


Figure 2. Variation in carbonate chemistry of platform water samples across a diurnal cycle on Caicos Platform. (a) [dissolved inorganic carbon], (b) total alkalinity (TA), (c) pH, (d) $p\text{CO}_2$, (e) Ω_{ar} , and (f) $\delta^{13}\text{C}_{\text{DIC}}$. Teal circles show measured values. Dashed gray horizontal lines show means for each data type in our data set, which is compared with means for each data type of Caicos Platform water previously (Trower et al., 2018) (dashed black line; samples from 2017). Dashed teal curves show diurnal engine model of the platform forced with κ_p estimate from our data. Vertical pink dashed lines indicate timing of civil dawn and dusk; vertical gray dash-dot lines indicate timing of high tide; vertical gray dashed lines indicate timing of low tide (only shown in panel b).

4. Discussion

Could the mismatch between the $\delta^{13}\text{C}_{\text{carb}}$ value predicted based on our field observations and bulk ooid $\delta^{13}\text{C}_{\text{carb}}$ values reflect that our data set is not representative of the full range of diurnal variability? For example, could seasonal differences in carbonate chemistry and productivity explain a relatively small diurnal variation observed during our sampling interval? Although there is no seasonal seawater carbonate chemistry data set for the Caicos

Platform, the Yucatan Peninsula can serve as a useful comparison as it is a relatively nearby carbonate platform with data. On the Yucatan Peninsula, Ω_{ar} varies by <0.2 , and [DIC] and alkalinity both vary by $<0.02 \text{ mmol/kg}$ (highest in the summer) (Gomez et al., 2020). Thus, we expect that any seasonal variations in seawater carbonate chemistry are likely to be much smaller in magnitude than our observed daily patterns. Comparison of diurnal versus seasonal patterns in seawater carbonate chemistry from Heron Island (a coral cay in the southern Great Barrier Reef) reveals that the magnitudes of shifts across the diurnal cycle stay relatively constant even as the values of mean pH [DIC], and alkalinity vary seasonally (Kline et al., 2015).

Could transiently higher productivity, temperature, or salinity on rare extreme days explain the discrepancy in predicted versus observed $\delta^{13}\text{C}_{\text{carb}}$ values? Although there can be seasonal variations in productivity of *Halimeda* and *Penicillus*, both taxa are most productive in summer (Payri, 1988; Wefer, 1980). Our sampling interval was in the summer (July), suggesting that our data set should reflect high productivity conditions for the Caicos Platform. Model sensitivity tests demonstrate that the photosynthetic forcing would need to be 4 times stronger ($\kappa_p \approx 550$ – $600 \mu\text{mol/kg}$, the maximum values observed in modern coral reefs) than observed during our sampling interval for the predicted $\delta^{13}\text{C}_{\text{carb}}$ value to match the observations (Figure S5 in Supporting Information S1). We observed a maximum platform water temperature of 31.7°C (Data Set S1); temperatures above 34 – 35°C strongly inhibit productivity of many tropical marine algae (Koch et al., 2013; Pratheepr et al., 2018; Wei et al., 2020), suggesting that warmer temperatures are implausible drivers of higher productivity. An additional set of model sensitivity tests show that, although warmer temperature could increase cumulative precipitation rate due to the temperature sensitivity of aragonite precipitation kinetics, this temperature effect would not result in a substantially different predicted $\delta^{13}\text{C}_{\text{carb}}$ value (Figure S6 in Supporting Information S1). Finally, although periods of enhanced evaporation could transiently increase Ω_{ar} values, results of an evaporative modeling sensitivity test demonstrate that the magnitudes of diurnal variations in cumulative $\delta^{13}\text{C}_{\text{carb}}$ values would be smaller at higher salinities for a given κ_p value (Figures S7 and S8 in Supporting Information S1). Even if we consider the cumulative effects of diurnal variations over longer timescales, where a few warmer, more productive days might occur, the diurnal engine model still cannot explain the difference between predicted versus observed $\delta^{13}\text{C}_{\text{carb}}$ values. For example, a single hot (35°C , the maximum before marine algal productivity is inhibited), extremely high productivity day ($\kappa_p = 600 \mu\text{mol/kg}$) during a month of “typical” summer days (e.g., what we observed during our sampling period) would increase the cumulative $\delta^{13}\text{C}_{\text{carb}}$ value by $<0.3\text{\textperthousand}$ relative to a month of only typical days (Figure S9 in Supporting Information S1). The effect of a rare hot and extremely productive day on the cumulative $\delta^{13}\text{C}_{\text{carb}}$ value is also increasingly diluted by subsequent typical summer days (Figure S9 in Supporting Information S1), so these rare days are only important if they are frequent (and, therefore, not rare). Thus, we conclude that our sample suite represents typical conditions on the Caicos Platform, and that daily or seasonal variations are an unlikely explanation for the significant mismatch between predicted and observed bulk $\delta^{13}\text{C}_{\text{carb}}$ values.

We assessed whether the ^{13}C Suess effect, in combination with the diurnal engine effect, might explain the offset between the $\delta^{13}\text{C}_{\text{carb}}$ value predicted by measured $\delta^{13}\text{C}_{\text{DIC}}$ values and the observed bulk and inner cortex $\delta^{13}\text{C}_{\text{carb}}$ value of Ambergris shoal ooids. Although the magnitude of the ^{13}C Suess effect has not been constrained specifically for the Caicos Platform, we consider that a shift of $\geq 1\text{\textperthousand}$ over the past 200 years is plausible (Figure 3c). Shallow water sclerosponges from Bahamas and Jamaica document a decrease in $\delta^{13}\text{C}_{\text{carb}}$ values of ca. $1.1\text{\textperthousand}$ from 1800 to 1995, a fingerprint of the ^{13}C Suess effect (Figure 3a) (Böhm et al., 2002; Lazareth et al., 2000; Swart et al., 2002). This rate of decrease has increased since 1960 (Figure 3a) (Böhm et al., 2002; Lazareth et al., 2000; Swart et al., 2002). Data from the Bermuda Atlantic Time-series Study (BATS) illustrate continuing declines in surface ocean $\delta^{13}\text{C}_{\text{DIC}}$ from $1.4\text{\textperthousand}$ in 1990 to $0.7\text{\textperthousand}$ in 2017 (Figure 3b) (Lueker et al., 1998). We compared the results for two endmember corrections to model predictions (Figures 3d–3f).

1. $0.8\text{\textperthousand}$, a conservative estimate of the magnitude of the ^{13}C Suess effect for this part of the ocean (Eide et al., 2017; Swart et al., 2010); and
2. $1.8\text{\textperthousand}$, consistent with the maximum plausible change in $\delta^{13}\text{C}_{\text{DIC}}$ values since 1,800 based on sclerosponge and BATS DIC data (Böhm et al., 2002; Lazareth et al., 2000; Lueker et al., 1998; Swart et al., 2002) (Figures 3a–3c).

Both scenarios increase the predicted cumulative $\delta^{13}\text{C}_{\text{carb}}$ values ($4.26\text{\textperthousand}$ for the first scenario, $5.26\text{\textperthousand}$ for the second scenario) (Figure 3f). We therefore interpret that the ^{13}C Suess effect could be responsible for a large component of the offset between predicted and observed bulk $\delta^{13}\text{C}_{\text{carb}}$ values on Caicos Platform. Given that ^{13}C

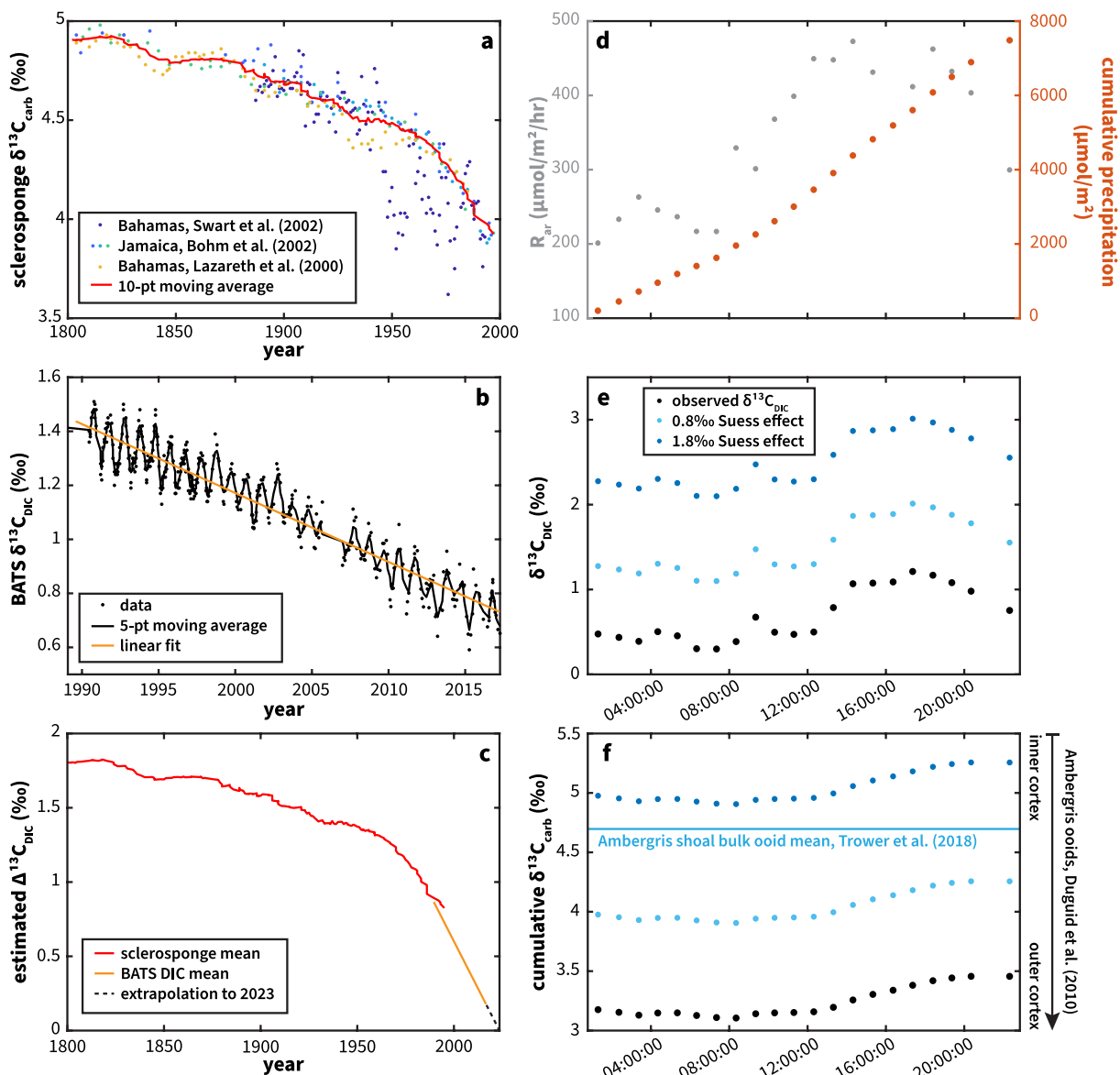


Figure 3. Evidence of the Suess effect for the Caicos Platform. (a) $\delta^{13}\text{C}_{\text{carb}}$ data from shallow water sclerosponges from locations in the Bahamas and Jamaica for the years 1800–2000 (Böhm et al., 2002; Lazareth et al., 2000; Swart et al., 2002); 10-pt moving average indicated by solid red line. (b) Bermuda Atlantic time-series study (BATS) $\delta^{13}\text{C}_{\text{DIC}}$ data for the years 1989–2017 (Lueker et al., 1998); 5-pt moving average indicated by solid black line, linear fit indicated by solid orange line. (c) Visualization of estimated total magnitude of the Suess effect in shallow seawater dissolved inorganic carbon (DIC) for the Caribbean ($\Delta^{13}\text{C}_{\text{DIC}}$) in 2023, combining the moving average from sclerosponge data (solid red line), the linear fit of BATS DIC data (solid orange line), and an extrapolation of the linear fit of the BATS data for the years 2018–2023 (dashed black line). (d) We used precipitation rates calculated based on observed Ω_{ar} values (left axis, gray points) to calculate cumulative precipitation across the diurnal cycle (right axis, orange points). (e) We compared observed $\delta^{13}\text{C}_{\text{DIC}}$ data (black points) with estimates corrected for a minimum and maximum magnitude of the Suess effect (0.8‰, light blue points, and 1.8‰, dark blue points, respectively). (f) We estimated cumulative $\delta^{13}\text{C}_{\text{carb}}$ using rates from (d) and different $\delta^{13}\text{C}_{\text{DIC}}$ estimates from (e). Note that since rates are normalized relative to total precipitation, the choice of kinetic rate parameters does not strongly affect the calculation. Arrow to the right of panel (f) illustrates ranges of $\delta^{13}\text{C}_{\text{carb}}$ values observed in sequential dissolution of the cortices of Ambergis shoal ooids, excluding outliers (flat line: ooid interior, arrow: ooid exterior) (Duguid et al., 2010).

Suess effect is observed in shallow water sclerosponges from the Bahamas, it seems likely that it also contributes to the gap between $\delta^{13}\text{C}_{\text{carb}}$ values of bulk ooid sand and modern $\delta^{13}\text{C}_{\text{DIC}}$ on the Great Bahama Bank.

This range of plausible magnitudes of the ^{13}C Suess effect for Ambergis shoal provides a novel explanation for the variation of $\delta^{13}\text{C}_{\text{carb}}$ between inner and outer cortices of Ambergis ooids previously reported by Duguid et al. (2010) (Figure 3f). We conclude that the outermost cortex $\delta^{13}\text{C}_{\text{carb}}$ values are consistent with carbonate precipitated in equilibrium with modern DIC, including the diurnal engine effect, which is in agreement with the

post-bomb radiocarbon ages of the outermost layers of Ambergris ooids requiring that those layers formed in the past 60 years (Duguid et al., 2010). In contrast, the inner cortex $\delta^{13}\text{C}_{\text{carb}}$ values are consistent with formation prior to the industrial revolution, in agreement with their pre-industrial radiocarbon ages. Importantly, this new explanation for $\delta^{13}\text{C}_{\text{carb}}$ patterns reported by Duguid et al. (2010) is still consistent with their interpretation that $\delta^{18}\text{O}_{\text{carb}}$ trends were driven by progressive recrystallization of an initial amorphous calcium carbonate (ACC) phase to aragonite; both isotope systems vary over time but through different mechanisms.

Trower et al. (2018) reported a trend in radiocarbon ages of ooids along the length of Ambergris shoal, implying that ooids farther west along the shoal have incorporated more young carbon because ooids are actively growing as they are transported along the shoal. One might therefore expect that bulk ooid $\delta^{13}\text{C}_{\text{carb}}$ values might decrease westward along shoal (due to the fingerprint of the ^{13}C Suess effect in the ooids with younger bulk ages), but the reported $\delta^{13}\text{C}_{\text{carb}}$ values are all within analytical certainty of each other (Trower et al., 2018). However, given available constraints on net growth rates of these ooids and the timescale of transport westward along the shoal, the magnitude of likely change in $\delta^{13}\text{C}_{\text{carb}}$ values is within the analytical uncertainty (Figure S10 in Supporting Information S1). This example illustrates why consideration of the ^{13}C Suess effect is critical: depending on the scale of measurement, it might not be obvious in “modern” sediments due to time-averaging.

Our data demonstrate a more muted diurnal cycle than observed in highly productive coral reef environments (Albright et al., 2015; Cyronak et al., 2013; Gattuso et al., 1997; Geyman & Maloof, 2019; Jokiel et al., 2014; McMahon et al., 2013; Nakamura & Nakamori, 2009; Richardson et al., 2017; Shaw et al., 2012, 2015; Suzuki et al., 1995). We expected that primary productivity in this setting would be less than in a reefal environment: the Caicos Platform is a wave-swept, grainy platform top with some calcifying algae and only sparse, small patch reefs. The low photosynthetic forcing for our study site (139 $\mu\text{mol}/\text{kg}$) is consistent with this intuition.

The muted diurnal engine effect on $\delta^{13}\text{C}_{\text{carb}}$ on Caicos Platform is also likely a consequence of the Ω_{ar} values we observed: Ω_{ar} ranged from 3.2 to 4.6 (mean 4.0) and was always strongly supersaturated ($\Omega_{\text{ar}} \gg 1$). This consistent supersaturation means that carbonate is precipitating throughout the diurnal cycle, albeit at rates that vary by approximately a factor of 2, and it does not dissolve in seawater overnight. This absence of net dissolution driven by $\Omega_{\text{ar}} < 1$ is an important difference in behavior relative to the general framework presented by Geyman and Maloof (2019) because it decreases the impact of diurnal variation in $\delta^{13}\text{C}_{\text{DIC}}$ values on $\delta^{13}\text{C}_{\text{carb}}$ values. Furthermore, consistently supersaturated Ω_{ar} values mean that rare days with a larger diurnal engine effect on $\delta^{13}\text{C}_{\text{carb}}$ values due to enhanced productivity and/or warmer temperatures are unlikely to substantially influence cumulative $\delta^{13}\text{C}_{\text{carb}}$ records because cumulative carbonate precipitation rates are not sufficiently different from typical days (Figure S9 in Supporting Information S1).

Our data not only provide evidence of the diurnal engine effect at play on a carbonate platform even in the absence of well-developed reef tracts, but also demonstrate that carbonate chemistry data sets from modern coral reefs are not necessarily representative of grainy platform settings like the Caicos Platform. Applying estimates of photosynthetic forcing derived from coral reef settings may lead to overestimation of the magnitude of the diurnal engine effect for a particular environment. At the same time, our data are also not necessarily broadly representative of all reef-poor shallow carbonate environments. We suggest that high-temporal-resolution carbonate chemistry data sets are needed from a wider variety of modern settings to better characterize the diversity of shallow carbonate environments, particularly to assess whether there are discernible relationships between photosynthetic communities (i.e., cyanobacteria vs. algae vs. corals) and factories of different carbonate sediment types (e.g., mud, ooids, skeletal grains). These data could then inform a facies-based approach to understanding in which ancient carbonate strata the diurnal engine effect is likely to be more significant and in which the effect is more muted.

Ultimately, assessing the extent and causes of modern $\delta^{13}\text{C}_{\text{carb}}$ variability apparently unrelated to global carbon cycle perturbation is a key step in validating or falsifying long-standing interpretations of Earth's $\delta^{13}\text{C}_{\text{carb}}$ records. These records span billions of years and have been used as archives of information about Earth's oxygenation, carbon cycle perturbations, and key events in the history of Earth and life. Our data suggest that some of the apparent inconsistency between $\delta^{13}\text{C}_{\text{carb}}$ and $\delta^{13}\text{C}_{\text{DIC}}$ values on modern carbonate platforms stems from time-averaging of $\delta^{13}\text{C}$ values across the recent, rapid carbon cycle perturbation induced by the industrial revolution. Modern carbonate sediments are key analogs for the ancient carbonate rock record, but contextualizing their anachronistic aspects is critical for appropriate and accurate applications of these analogies to deep time.

5. Inclusion in Global Research

We thank the Department of Environment and Coastal Resources (DECR) of Turks and Caicos Islands government and the Turks and Caicos National Trust for granting a research permit to perform this work. Results of this research are incorporated into outreach and education material that we create for DECR as a condition of this research permit. We also thank Shaun Austin, Paul Mahoney, and James Seymour for their invaluable logistical support with fieldwork.

Data Availability Statement

All previously published data are available in Lazareth et al. (2000), Bohm et al. (2002), and Swart et al. (2002). Water chemistry data and all code necessary to run models and generate figures are available in Trower (2024).

Acknowledgments

The authors thank Laura Liermann and the PSU LIME Lab for assistance with ion concentration analyses; and Ashley Maloney and CUBES-SIL (RRID: SCR_019300) for assistance with $\delta^{13}\text{C}_{\text{DIC}}$ analyses. This work was supported by NSF Grants OCE-2032129 (to EJT and MLG) and OCE-2307830 (to EJT, MLG, and MDC), and ACS PRF Grant 62161-DNI2 (to EJT). Publication of this article was funded by the University of Colorado Boulder Libraries Open Access Fund. We are grateful for constructive reviews by Peter Swart, Adam Maloof, Emily Geyman, Bolton Howes, Julia Wileots, and one anonymous reviewer.

References

Ahm, A.-S. C., Bjerrum, C. J., Blättler, C. L., Swart, P. K., & Higgins, J. A. (2018). Quantifying early marine diagenesis in shallow-water carbonate sediments. *Geochimica et Cosmochimica Acta*, 236, 140–159. <https://doi.org/10.1016/j.gca.2018.02.042>

Albright, R., Benthuyzen, J., Cantin, N., Caldeira, K., & Anthony, K. (2015). Coral reef metabolism and carbon chemistry dynamics of a coral reef flat. *Geophysical Research Letters*, 42(10), 3980–3988. <https://doi.org/10.1002/2015gl063488>

Beaupré, S. R., Roberts, M. L., Burton, J. R., & Summons, R. E. (2015). Rapid, high-resolution ^{14}C chronology of ooids. *Geochimica et Cosmochimica Acta*, 159, 126–138. <https://doi.org/10.1016/j.gca.2015.03.009>

Bohm, F., Haase-Schramm, A., Eisenhauer, A., Dullo, W.-C., Joachimski, M. M., Lehnert, H., & Reitner, J. (2002). Evidence for preindustrial variations in the marine surface water carbonate system from coralline sponges. *Geochemistry, Geophysics, Geosystems*, 3(3), 1–13. <https://doi.org/10.1029/2001gc000264>

Burton, E. A., & Walter, L. M. (1987). Relative precipitation rates of aragonite and Mg calcite from seawater: Temperature or carbonate ion control? *Geology*, 15(2), 111–114. [https://doi.org/10.1130/0091-7613\(1987\)15<111:rpa>2.0.co;2](https://doi.org/10.1130/0091-7613(1987)15<111:rpa>2.0.co;2)

Cyronak, T., Santos, I. R., McMahon, A., & Eyre, B. D. (2013). Carbon cycling hysteresis in permeable carbonate sands over a diel cycle: Implications for ocean acidification. *Limnology & Oceanography*, 58(1), 131–143. <https://doi.org/10.4319/lo.2013.58.1.01031>

Dravis, J. J., & Wanless, H. R. (2017). Impact of strong easterly trade winds on carbonate petroleum exploration—relationships developed from Caicos Platform, Southeastern Bahamas. *Marine and Petroleum Geology*, 85, 272–300. <https://doi.org/10.1016/j.marpetgeo.2017.04.010>

Duguid, S. M. A., Kurtis Kyser, T., James, N. P., & Rankey, E. C. (2010). Microbes and Ooids. *Journal of Sedimentary Research*, 80(3), 236–251. <https://doi.org/10.2110/jssr.2010.027>

Eide, M., Olsen, A., Ninnemann, U. S., & Eldevik, T. (2017). A global estimate of the full oceanic ^{13}C Suess effect since the preindustrial. *Global Biogeochemical Cycles*, 31(3), 492–514. <https://doi.org/10.1002/2016gb005472>

Gattuso, J.-P., Payri, C. E., Pichon, M., Delesalle, B., & Frankignoulle, M. (1997). Primary production, calcification, and air-sea CO_2 fluxes of a Macroalgal-dominated coral reef community (Moorea, French Polynesia). *Journal of Phycology*, 33(5), 729–738. <https://doi.org/10.1111/j.0022-3646.1997.00729.x>

Geyman, E. C., & Maloof, A. C. (2019). A diurnal carbon engine explains ^{13}C -enriched carbonates without increasing the global production of oxygen. *Proceedings of the National Academy of Sciences of the United States of America*, 116(49), 24433–24439. <https://doi.org/10.1073/pnas.1908783116>

Geyman, E. C., & Maloof, A. C. (2021). Facies control on carbonate $\delta^{13}\text{C}$ on the great Bahama Bank. *Geology*, 49(9), 1049–1054. <https://doi.org/10.1130/g48862.1>

Gomez, F. A., Wanninkhof, R., Barbero, L., Lee, S.-K., & Hernandez, F. J., Jr. (2020). Seasonal patterns of surface inorganic carbon system variables in the Gulf of Mexico inferred from a regional high-resolution ocean biogeochemical model. *Biogeosciences*, 17(6), 1685–1700. <https://doi.org/10.5194/bg-17-1685-2020>

Higgins, J. A., Blättler, C. L., Lundstrom, E. A., Santiago-Ramos, D. P., Akhtar, A. A., Crüger Ahm, A.-S., et al. (2018). Mineralogy, early marine diagenesis, and the chemistry of shallow-water carbonate sediments. *Geochimica et Cosmochimica Acta*, 220, 512–534. <https://doi.org/10.1016/j.gca.2017.09.046>

Ingalls, M., Frantz, C. M., Snell, K. E., & Trower, E. J. (2020). Carbonate facies-specific stable isotope data record climate, hydrology, and microbial communities in Great Salt Lake, UT. *Geobiology*, 18(5), 566–593. <https://doi.org/10.1111/gbi.12386>

Jokiel, P. L., Jury, C. P., & Rodgers, K. S. (2014). Coral-algae metabolism and diurnal changes in the CO_2 -carbonate system of Bulk sea water. *PeerJ*, 2, e378. <https://doi.org/10.7717/peerj.378>

Jury, M. R. (2013). Turks and Caicos Islands climate and its impacts. *Earth Interactions*, 17(18), 1–20. <https://doi.org/10.1175/2012ie000490.1>

Keeling, C. D. (1979). The Suess effect: ^{13}C -Carbon– ^{14}C Carbon interrelations. *Environment International*, 2(4), 229–300. [https://doi.org/10.1016/0160-4120\(79\)90005-9](https://doi.org/10.1016/0160-4120(79)90005-9)

Kline, D. I., Teneva, L., Hauri, C., Schneider, K., Miard, T., Chai, A., et al. (2015). Six month in situ high-resolution carbonate chemistry and temperature study on a coral reef flat reveals asynchronous pH and temperature anomalies. *PLoS One*, 10(6), e0127648. <https://doi.org/10.1371/journal.pone.0127648>

Knoll, A. H., Hayes, J. M., Kaufman, A. J., Swett, K., & Lambert, I. B. (1986). Secular variation in carbon isotope ratios from Upper Proterozoic successions of Svalbard and East Greenland. *Nature*, 321(6073), 832–838. <https://doi.org/10.1038/321832a0>

Koch, M., Bowes, G., Ross, C., & Zhang, X.-H. (2013). Climate change and ocean acidification effects on seagrasses and marine macroalgae. *Global Change Biology*, 19(1), 103–132. <https://doi.org/10.1111/j.1365-2486.2012.02791.x>

Kump, L. R., & Arthur, M. A. (1999). Interpreting carbon-isotope excursions: Carbonates and organic matter. *Chemical Geology*, 161(1), 181–198. [https://doi.org/10.1016/s0009-2541\(99\)00086-8](https://doi.org/10.1016/s0009-2541(99)00086-8)

Lazareth, C. E., Willenz, P., Navez, J., Keppens, E., Dehairs, F., & André, L. (2000). Sclerosponges as a new potential recorder of environmental changes: Lead in *Ceratoporella nicholsoni*. *Geology*, 28(6), 515–518. [https://doi.org/10.1130/0091-7613\(2000\)28<515:saanpr>2.0.co;2](https://doi.org/10.1130/0091-7613(2000)28<515:saanpr>2.0.co;2)

Logan, A., & Sealey, K. S. (2013). The reefs of the Turks and Caicos Islands. In C. R. C. Sheppard (Ed.), *Coral reefs of the United Kingdom overseas territories* (pp. 97–114). Springer.

Lueker, T. J., Keeling, C. D., Guenther, P. R., Whalen, M., & Mook, W. G. (1998). Inorganic carbon variations in surface ocean water near Bermuda [Dataset]. *Scripps Oceanography*. <https://escholarship.org/uc/item/8742p2nb>

McMahon, A., Santos, I. R., Cyronak, T., & Eyre, B. D. (2013). Hysteresis between coral reef calcification and the seawater aragonite saturation state. *Geophysical Research Letters*, 40(17), 4675–4679. <https://doi.org/10.1002/grl.50802>

Nakamura, T., & Nakamori, T. (2009). Estimation of photosynthesis and calcification rates at a fringing reef by accounting for diurnal variations and the zonation of coral reef communities on reef flat and slope: A case study for the Shiraho reef, Ishigaki Island, Southwest Japan. *Coral Reefs*, 28(1), 229–250. <https://doi.org/10.1007/s00338-008-0454-8>

Oehlert, A. M., & Swart, P. K. (2014). Interpreting carbonate and organic carbon isotope covariance in the sedimentary record. *Nature Communications*, 5(1), 4672. <https://doi.org/10.1038/ncomms5672>

Parkhurst, D. L., & Appelo, C. A. J. (2013). *Description of input and examples for PHREEQC version 3—a computer program for speciation, batch-reaction, one-dimensional transport, and inverse geochemical calculations* (No. Techniques and methods 6–A43). USGS.

Payri, C. E. (1988). *Halimeda* contribution to organic and inorganic production in a Tahitian reef system. *Coral Reefs*, 6(3), 251–262. <https://doi.org/10.1007/bf00302021>

Prathee, A., Kaebsrikhaw, R., Mayakun, J., & Darakrai, A. (2018). The effects of light intensity and temperature on the calcification rate of *Halimeda macroloba*. *Journal of Applied Phycology*, 30(6), 3405–3412. <https://doi.org/10.1007/s10811-018-1534-y>

Present, T. M., Gomes, M. L., Trower, E. J., Stein, N. T., Lingappa, U. F., Naviaux, J., et al. (2021). Non-lithifying microbial ecosystem dissolves peritidal lime sand. *Nature Communications*, 12(1), 3037. <https://doi.org/10.1038/s41467-021-23006-1>

Purkis, S. J., Harris, P. M., & Ellis, J. (2012). Patterns of sedimentation in the contemporary red sea as an analog for ancient carbonates in rift settings. *Journal of Sedimentary Research*, 82(11), 859–870. <https://doi.org/10.2110/jsr.2012.77>

Purkis, S. J., Rowlands, G. P., & Kerr, J. M. (2015). Unravelling the influence of water depth and wave energy on the facies diversity of shelf carbonates. *Sedimentology*, 62(2), 541–565. <https://doi.org/10.1111/sed.12110>

Richardson, C. M., Dulai, H., Popp, B. N., Ruttnerberg, K., & Fackrell, J. K. (2017). Submarine groundwater discharge drives biogeochemistry in two Hawaiian reefs. *Limnology & Oceanography*, 62(S1), S348–S363. <https://doi.org/10.1002/lno.10654>

Romanek, C. S., Grossman, E. L., & Morse, J. W. (1992). Carbon isotopic fractionation in synthetic aragonite and calcite: Effects of temperature and precipitation rate. *Geochimica et Cosmochimica Acta*, 56(1), 419–430. [https://doi.org/10.1016/0016-7037\(92\)90142-6](https://doi.org/10.1016/0016-7037(92)90142-6)

Sharp, J. D., Pierrot, D., Humphreys, M. P., Epitalon, J.-M., Orr, J. C., Lewis, E. R., & Wallace, D. W. R. (2023). CO2SYSv3 for MATLAB (version 3.2.1.0) [Matlab]. <https://doi.org/10.5281/ZENODO.3950563>

Shaw, E. C., McNeil, B. I., & Tilbrook, B. (2012). Estimation of photosynthesis and calcification rates at a fringing reef by accounting for diurnal variations and the zonation of coral reef communities on reef flat and slope: A case study for the Shiraho reef, Ishigaki Island, Southwest Japan. *Journal of Geophysical Research*, 117(C3), C03038. <https://doi.org/10.1029/2011jc007655>

Shaw, E. C., Phinn, S. R., Tilbrook, B., & Steven, A. (2015). Natural in situ relationships suggest coral reef calcium carbonate production will decline with ocean acidification. *Limnology & Oceanography*, 60(3), 777–788. <https://doi.org/10.1002/lno.10048>

Smith, M. E., & Swart, P. K. (2022). The influence of diagenesis on carbon and oxygen isotope values in shallow water carbonates from the Atlantic and Pacific: Implications for the interpretation of the global carbon cycle. *Sedimentary Geology*, 434(106147), 106147. <https://doi.org/10.1016/j.sedgeo.2022.106147>

Suess, H. E. (1955). Radiocarbon concentration in modern wood. *Science*, 122(3166), 415–417. <https://doi.org/10.1126/science.122.3166.415.b>

Suzuki, A., Nakamori, T., & Kayanne, H. (1995). The mechanism of production enhancement in coral reef carbonate systems: Model and empirical results. *Sedimentary Geology*, 99(3), 259–280. [https://doi.org/10.1016/0037-0738\(95\)00048-d](https://doi.org/10.1016/0037-0738(95)00048-d)

Swart, P. K. (2015). The geochemistry of carbonate diagenesis: The past, present and future. *Sedimentology*, 62(5), 1233–1304. <https://doi.org/10.1111/sed.12205>

Swart, P. K., & Eberli, G. (2005). The nature of the $\delta^{13}\text{C}$ of periplatform sediments: Implications for stratigraphy and the global carbon cycle. *Sedimentary Geology*, 175(1), 115–129. <https://doi.org/10.1016/j.sedgeo.2004.12.029>

Swart, P. K., Greer, L., Rosenheim, B. E., Moses, C. S., Waite, A. J., Winter, A., et al. (2010). The $\delta^{13}\text{C}$ Suess effect in Scleractinian corals mirror changes in the anthropogenic CO_2 inventory of the surface oceans. *Geophysical Research Letters*, 37(5), L05604. <https://doi.org/10.1029/2009gl041397>

Swart, P. K., & Oehlert, A. M. (2018). Revised interpretations of stable C and O patterns in carbonate rocks resulting from meteoric diagenesis. *Sedimentary Geology*, 364, 14–23. <https://doi.org/10.1016/j.sedgeo.2017.12.005>

Swart, P. K., Reijmer, J. J. G., & Otto, R. (2009). A re-evaluation of facies on great Bahama bank II: Variations in the $\delta^{13}\text{C}$, $\delta^{18}\text{O}$ and mineralogy of surface sediments. In P. K. Swart, G. P. Eberli, & J. A. McKenzie (Eds.), *Perspectives in carbonate geology: A tribute to the career of robert nathan ginsburg* (pp. 47–59). Wiley-Blackwell.

Swart, P. K., Thorrold, S., Rosenheim, B., Eisenhauer, A., Harrison, C. G. A., Grammer, M., & Latkoczy, C. (2002). Intra-annual variation in the stable Oxygen and Carbon and trace element composition of sclerosponges. *Paleoceanography and Paleoclimatology*, 17(3), 1045. <https://doi.org/10.1029/2000pa000622>

Trower, E. J. (2024). Caicos Platform C isotope model, v1.2 (Version 1.1) [Matlab]. <https://doi.org/10.5281/zenodo.11068313>

Trower, E. J., Cantine, M. D., Gomes, M. L., Grotzinger, J. P., Knoll, A. H., Lamb, M. P., et al. (2018). Active ooid growth driven by sediment transport in a high-energy shoal, Little Ambergris cay, Turks and Caicos Islands. *Journal of Sedimentary Research*, 88(9), 1132–1151. <https://doi.org/10.2110/jsr.2018.59>

Wefer, G. (1980). Carbonate production by algae *Halimeda*, *Penicillus* and *Padina*. *Nature*, 285(5763), 323–324. <https://doi.org/10.1038/285323a0>

Wei, Z., Mo, J., Huang, R., Hu, Q., Long, C., Ding, D., et al. (2020). Physiological performance of three calcifying green macroalgae *Halimeda* species in response to altered seawater temperatures. *Acta Oceanologica Sinica*, 39(2), 89–100. <https://doi.org/10.1007/s13131-019-1471-3>

Zachos, J., Pagani, M., Sloan, L., Thomas, E., & Billups, K. (2001). Trends, rhythms, and aberrations in global climate 65 Ma to present. *Science*, 292(5517), 686–693. <https://doi.org/10.1126/science.1059412>

References From the Supporting Information

Gomes, M. L., Riedman, L. A., O'Reilly, S., Lingappa, U., Metcalfe, K., Fike, D. A., et al. (2020). Taphonomy of biosignatures in microbial mats on Little Ambergris cay, Turks and Caicos Islands. *Frontiers of Earth Science*, 8, 387. <https://doi.org/10.3389/feart.2020.576712>

Lazar, B., Starinsky, A., Katz, A., Sass, E., & Ben-Yaakov, S. (1983). The carbonate system in hypersaline solutions: Alkalinity and CaCO_3 solubility of evaporated seawater. *Limnology & Oceanography*, 28(5), 978–986. <https://doi.org/10.4319/lo.1983.28.5.00978>

Lingappa, U. F., Stein, N. T., Metcalfe, K. S., Present, T. M., Orphan, V. J., Grotzinger, J. P., et al. (2022). Early impacts of climate change on a coastal marine microbial mat ecosystem. *Science Advances*, 8(21), eabm7826. <https://doi.org/10.1126/sciadv.abm7826>

McCaffrey, M. A., Lazar, B., & Holland, H. D. (1987). The evaporation path of seawater and the coprecipitation of Br- and K+ with halite. *Journal of Sedimentary Research*, 57(5), 928–937. <https://doi.org/10.1306/212f8cab-2b24-11d7-8648000102c1865d>

Stein, N. T., Grotzinger, J. P., Quinn, D. P., Lingappa, U. F., Present, T. M., Trower, E. J., et al. (2023). Geomorphic and environmental controls on microbial mat fabrics on Little Ambergris cay, Turks and Caicos Islands. *Sedimentology*, 70(6), 1915–1944. <https://doi.org/10.1111/sed.13100>

Trembath-Reichert, E., Ward, L. M., Slotnick, S. P., Bachtel, S. L., Kerans, C., Grotzinger, J. P., & Fischer, W. W. (2016). Gene sequencing-based analysis of microbial-mat morphotypes, Caicos platform, British West indies. *Journal of Sedimentary Research*, 86(6), 629–636. <https://doi.org/10.2110/jsr.2016.40>